Nucleic Acids Research, 1999, Vol. 27, No. 5 **1283–1288**

The exosome subunit Rrp43p is required for the efficient maturation of 5.8S, 18S and 25S rRNA

Nilson I. T. Zanchin and David S. Goldfarb*

Department of Biology, University of Rochester, Rochester, NY 14627, USA

Received November 28, 1998; Revised and Accepted January 15, 1999

ABSTRACT

The *Saccharomyces cerevisiae* protein Rrp43p co-purifies with four other 3′→5′ exoribonucleases in a complex that has been termed the exosome. Rrp43p itself is similar to prokaryotic RNase PH. Individual exosome subunits have been implicated in the 3′ maturation of the 5.8S rRNA found in 60S ribosomes and the 3′ degradation of mRNAs. However, instead of being deficient in 60S ribosomes, Rrp43p-depleted cells were deficient in 40S ribosomes. Pulse–chase and steady-state northern analyses of pre-RNA and rRNA levels revealed a significant delay in the synthesis of both 25S and 18S rRNAs, accompanied by the stable accumulation of 35S and 27S pre-rRNAs and the under-accumulation of 20S pre-rRNA. In addition, Rrp43p-depleted cells accumulated a 23S aberrant pre-rRNA and a fragment excised from the 5′ ETS. Therefore, in addition to the maturation of 5.8S rRNA, Rrp43p is required for the maturation 18S and 25S rRNA.

INTRODUCTION

In eukaryotes, three of the four rRNAs (18S, 5.8S and 25–28S) are synthesized from a single pre-rRNA that is transcribed by RNA polymerase I. rRNA maturation involves digestion of the spacer sequences and modifications that include ribose and base methylation and conversion of uridine to pseudouridine (for reviews see 1–4). Whereas the mechanism of pre-rRNA processing still remains largely unknown, the major steps of the processing pathway in *Saccharomyces cerevisiae* have been established (1,2; see also Fig. 1). Briefly, processing of the 35S pre-rRNA starts with removal of the 5′ ETS followed by the first cleavage in ITS1 (site A_2). These processing steps, which separate 20S pre-rRNA from 27S pre-RNA, require the same set of nucleolar proteins and small nucleolar RNAs (snoRNAs) (1). The 20S pre-rRNA is incorporated into 40S subunits and converted to 18S rRNA in the cytoplasm (5). The 5′-end of 27S pre-rRNA is processed by divergent pathways (1,6). Approximately 90% of 27S pre-rRNA is cleaved at A_3 in ITS1 and processed to 25S and $5.8S_S$ rRNA and the remainder is processed to 25S and $5.8S_L$ rRNA. The form $5.8S_L$ contains 8–10 extra residues at the 5′-end as compared with the $5.8S_S$ form.

In *S.cerevisiae*, a relatively large number of non-ribosomal factors have been implicated in ribosome biogenesis. These factors include nucleolar proteins, snoRNAs, putative RNA helicases and a number of nucleases (1–4,6–8). Rnt1p, which is similar to prokaryotic RNase III, and the RNase MRP show specific endonucleolytic activities *in vitro* (9,10). Rnt1p has been implicated in cleavages in the 5′ ETS (site A_0) and in the 3′ ETS (9). RNase MRP is responsible for cleavage of 27S pre-rRNA at A_3 (10). Processing of the resulting $27SA_3$ pre-rRNA to form the mature 5′-end of the $5.8S_S$ requires the 5′→3′ exonucleases Rat1p and Xrn1p (6,8). These nucleases are also required for degradation of excised spacer fragments, including the sections between A_0 and A_1, A_2 and A_3, and D and A_2 (1,6,8).

Although factors involved in the initial cleavage of 27S pre-rRNA in ITS2 have not been identified, a number of genes have been implicated in the 3′→5′ exoribonucleolytic processing of 5.8S rRNA, which occurs after cleavage at C_2 (Fig. 1). Five proteins, Rrp4p, Rrp41p/Ski6p, Rrp42p, Rrp43p and Rrp44p/Dis3p, comprise a complex called the exosome that has been implicated in 5.8S processing (7,11). Rrp4p, Rrp41p/Ski6p and Rrp44p/Dis3p exhibit *in vitro* 3′→5′ exoribonuclease activity (7). Rrp42p and Rrp43p are similar to the RNase PH/PNPase family of ribonucleases and, for this reason, are also presumed to be 3′→5′ exoribonucleases (7,12). Depletion of any of the five exosome subunits delays 5.8S maturation and results in the accumulation of 7S pre-rRNA and an array of 5.8S rRNAs with extended 3′-tails (7). The *ski6-2* mutant accumulates a novel 38S particle containing 5′-truncated 25S rRNA but no 5.8S rRNA (13). Deficiencies in an additional gene, *RRP6*, which is similar to RNase D, cause the accumulation of 5.8S rRNAs with short 3′-end extensions (14). The exosome subunits Rrp4p and Rrp41p/Ski6p have also been implicated in the 3′ degradation of mRNAs (15).

We previously described the characterization of *NIP7*, a conserved *S.cerevisiae* gene that is required for pre-rRNA processing and 60S subunit biogenesis (16). Rrp43p and a novel protein, Nop8p, were subsequently identified as Nip7p-interacting proteins (Zanchin and Goldfarb, in press). In order to determine whether there is a functional interaction between Nip7p and Rrp43p, we performed a pre-rRNA processing analysis in Rrp43p-depleted cells. While these results confirm the proposed role of Rrp43p in the 3′ maturation of 5.8S rRNA (7), they provide strong evidence for additional roles in the maturation of 18S and 25S rRNAs. We conclude that Rrp43p, and by inference the exosome, is required for the maturation of 5.8S, 18S and 25S rRNAs.

*To whom correspondence should be addressed. Tel: +1 716 275 3890; Fax: +1 716 275 2070; Email: dasg@uhura.cc.rochester.edu

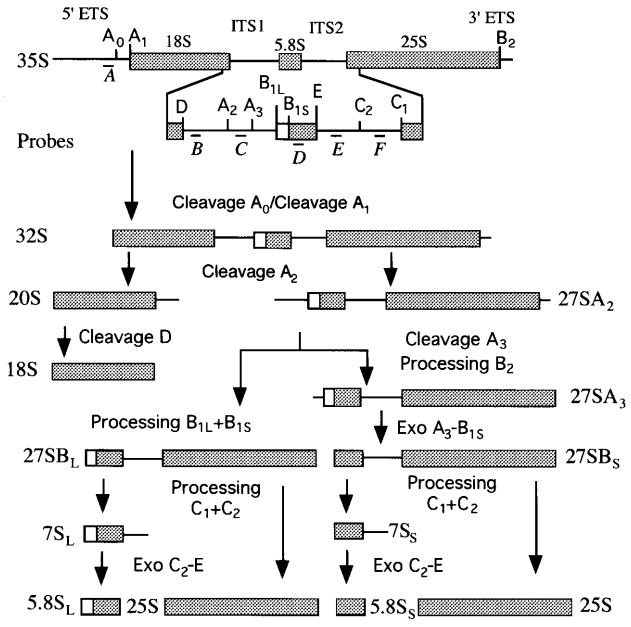

Figure 1. Structure of the 35S pre-rRNA and major intermediates of the rRNA processing pathway in *S.cerevisiae*. The 35S pre-rRNA contains the sequences of the mature 18S, 5.8S and 25S rRNAs separated by two internal transcribed spacers (ITS1 and ITS2) and flanked by 5′ and 3′ external transcribed spacers (ETS). Letters below the 35S pre-rRNA diagram (probes A–F) indicate the position of the oligonucleotide probes used in northern analysis.

MATERIALS AND METHODS

DNA analysis methods and plasmid construction

DNA cloning and electrophoresis analyses were performed as described by Sambrook *et al*. (17). DNA sequencing was performed using the Big Dye method (Perkin Elmer). Plasmid YCpGAL-RRP43 contains two IgG-binding domains of the *Staphyllococcus aureus* protein A fused to the N-terminus of Rrp43p under the control of the *GAL1* promoter. Vector YCpGAL-RRP43 was constructed by inserting the *GAL1* promoter digested with *Eco*RI and *Sal*I, the protein A epitope tag digested with *Nde*I–*Xba*I and the RRP43 ORF digested with *Xba*I–*Sal*I into the vector YCplac33 (18) cleaved with *Eco*RI and *Sal*I.

Yeast strains, media and genetic techniques

Growth and genetic analysis of yeast strains was performed as described by Sherman *et al*. (19,20). Various carbon sources were added to YP (yeast extract and peptone) and SC (synthetic complete) media. YPD/SCglu and YPgal/SCgal media contained either 2% glucose or 1% galactose plus 1% raffinose, respectively, as carbon source. Yeast strain DG458 (MAT**a** *ade2-1 leu2-3,112 his3-11,15 trp1-1 ura3-1 can1-100 rrp43*::*KAN* p[URA3 GAL::PrtA::RRP43]) was constructed by transforming haploid W303-1a cells carrying vector YCpGAL-RRP43 with a PCR-amplified *KAN* gene as described by Güldener *et al*. (21). The sequences of the primers used for amplification of the *KAN* gene are: 5′-ACAGTAGTTTCACAGGCATCTAATATTGGAAAT-GGCTGAAAGTACCAGCTGAAGCTTCGTACGC-3′ for the 5′ primer and 5′-TCCGAGTCTTTTATATGTTAAATCTTGTTG-ACAAATCGTCCGCTCGCATAGGCGACTAGTGGATCTG-3′ for the 3′ primer. The parental strain W303-1a (MAT**a** *ade2-1 leu2-3,112 his3-11,15 trp1-1 ura3-1 can1-100*) was used as a control.

Polysome profile analysis

Polysome profiles were analyzed as described previously (16). Briefly, cell extracts were isolated from 300 ml YPgal cultures grown to mid-exponential phase or from cells grown to mid-exponential phase (OD_{600} between 0.4 and 0.6) in YPgal and shifted to YPD for 12 h. Cycloheximide was added to the cultures (100 µg/ml), cells were harvested by centrifugation and resuspended in 0.5 ml of breaking buffer [20 mM HEPES–KOH, pH 7.4, 2 mM $Mg(OAc)_2$, 100 mM KCl, 1 mM DTT, 1 mM PMSF, 100 µg/ml cycloheximide]. Cells were disrupted by vortexing with 1 vol of glass beads and extracts were cleared by centrifugation (8000 *g*) for 5 min at 4°C. Aliquots of 20 OD_{254} of extract were loaded on 15–50% gradients and polysomes separated by centrifugation at 40 000 r.p.m. for 4 h at 4°C using a Beckman SW41 rotor. Gradients were fractionated using a Buchler Auto-densiflow IIC fractionator and monitored at 254 nm using a UA-5 absorbance/fluorescence monitor (ISCO).

rRNA analyses

Metabolic labeling of rRNA was performed as described previously (16,22). Exponentially growing cultures of W303-1a (*RRP43*) and DG458 (*GAL*::*RRP43*) were shifted from SCgal to SCglu lacking methionine and incubated at 30°C for 8 h. Subsequently, cells were pulse–chase-labeled with 100 µCi/ml [methyl-^{3}H]methionine (DuPont-NEN) for 2 min and chased with 100 µg/ml unlabeled methionine. At various times, samples were taken and quickly frozen in a dry ice/ethanol bath. Total RNA was isolated from yeast cells using the hot phenol method (23) and separated by electrophoresis on 1.2% agarose–6% formaldehyde gels (17). Subsequently, gels were incubated in EnHance (Amersham) and submitted to autoradiography.

For analysis of pre-rRNA steady-state levels, RNA was isolated from strains W303-1a and DG458 incubated in YPgal or shifted to YPD. Samples were collected for RNA extraction at times 0 and 12 h after the shift to YPD for W303-1a and at times 0, 4, 8 and 12 h after the shift to YPD for DG458. Following electrophoresis on 1.2% agarose–6% formaldehyde gels, RNA was transferred by northern blot to Hybond nylon membranes (Amersham) as described (17). Membranes were probed with ^{32}P-labeled oligonucleotides complementary to specific regions of the 35S pre-rRNA, using the hybridization conditions described previously (16) and submitted to autoradiography. The oligonucleotide probes used (see also Fig. 1) were: 5′-GGTCTCTCT-GCTGCCGGAAATG-3′ (probe A); 5′-GCTCTCATGCTCTT-GCCAAAAC-3′ (probe B); 5′-TGTTACCTCTGGGCCCCG-3′ (probe C); 5′-CGTATCGCATTTCGCTGCGTTC-3′ (probe D); 5′-GGCCAGCAATTTCAAGTTAAC-3′ (probe E); and 5′-GT-TCGCCTAGACGCTCTCTTC-3′ (probe F).

RESULTS

Construction of an *RRP43* conditional strain

A complete gene replacement of *RRP43* was produced by transforming haploid W303-1a carrying vector YCpGAL-RRP43

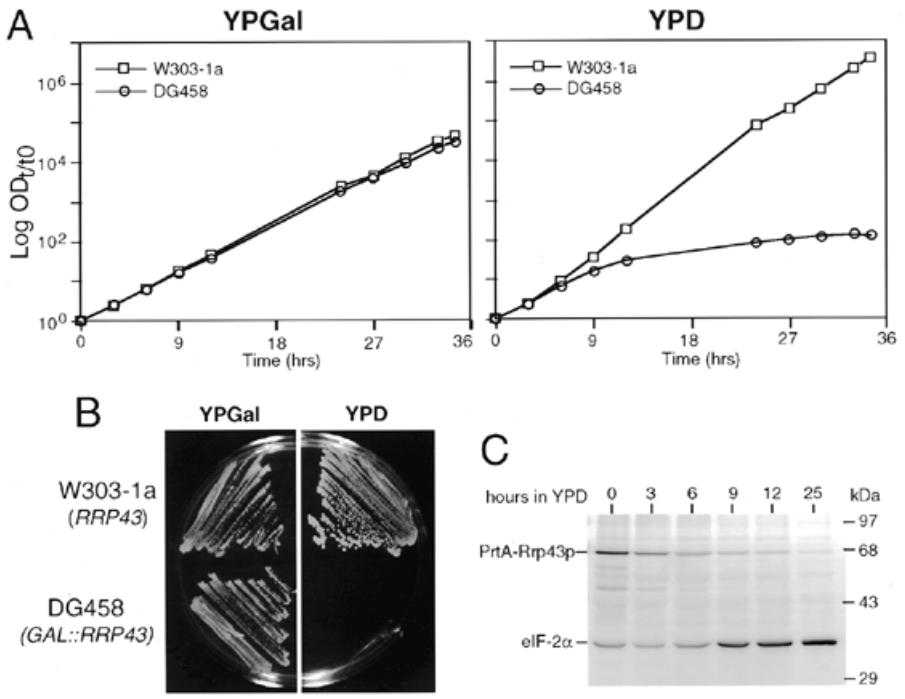

Figure 2. Characterization of the conditional strain for RRP43. (**A**) Growth curves of W303-1a (*RRP43*) and DG458 (*GAL*::*RRP43*) cultured at 30°C in YPGal and shifted to YPD at time 0. OD_{600} values are plotted as log OD_t/t_0, where t_0 is the initial OD_{600} and t is time in hours after transfer to YPD. (**B**) Growth at 30°C of W303-1a and DG456 on YPGal and YPD plates. (**C**) Immunoblot analysis showing levels of PrtA-Rrp43p and endogenous eIF2α in DG458 at various times after a shift from YPGal to YPD. The same amount of total protein was loaded in each lane. See Materials and Methods for details.

with a PCR-amplified *KAN* gene targeted for insertion into *RRP43* by using the method described by Güldener *et al.* (21; see Materials and Methods). Insertion of the *KAN* gene into the *RRP43* gene was confirmed by PCR analysis (not shown). Growth of *kan*^{r} transformants was dependent on galactose (Fig. 2A and B), indicating that growth was dependent on the *GAL1-RRP43* gene carried by the vector YCpGAL-RRP43. This result is consistent with a previous report that *RRP43* is an essential gene (7). One of the *kan*^{r} transformants (DG458) was further characterized. DG458 (*GAL*::*RRP43*) and control W303-1a (*RRP43*) cells grew similarly on galactose (Fig. 2A and B), however, DG458 did not grow on glucose plates (Fig. 2B). The growth of DG458 cells after a shift from galactose to glucose liquid medium slowed beginning at ~6 h and was severely impeded by 10–12 h (Fig. 2A). The reduction in the growth rate of DG458 cells on glucose correlated with the decrease in cellular levels of PrtA-Rrp43p as determined by immunoblot analysis (Fig. 2C). In contrast to the effect of glucose on PrtA-Rrp43p levels, the levels of an internal control protein, eIF-2α, increased during the same time course (Fig. 2C). Because increased expression of eIF-2α after shift from YPGal to YPD has been observed in other genetic backgrounds, this effect is most likely due to the carbon source and not to Rrp43p depletion.

Depletion of Rrp43p reduces cellular 40S/60S subunit ratio

Polysome analysis can provide a diagnostic overview of the composition and activity of the cellular translational apparatus. Extracts were prepared from DG458 (*GAL*::*RRP43*) and control W303-1a (*RRP43*) cells maintained in galactose or shifted to glucose for 12 h. As shown in Figure 3A and B, the polysome profiles from galactose-grown DG458 and W303-1a cells were similar, although DG458 cells contained somewhat lower levels of polysomes. In contrast, the polysome profile of glucose-grown DG458 cells was strikingly different from that of W303-1a cells (Fig. 3C and D). Specifically, the polysome profile of extracts from Rrp43p-depleted cells displayed a significant reduction in the level of free 40S subunits, an increase in free 60S subunits and a decrease in the total amount of polysomes (Fig. 3D). Rrp43p was previously implicated in 5.8S rRNA processing (7), which would be expected to result in a deficit of 60S rather than 40S subunits. These results suggest that Rrp43p has a primary function in 40S ribosome biogenesis.

Pre-rRNA processing is defective in Rrp43p-depleted cells

Although Rrp43p was previously implicated in the processing of 5.8S rRNA, the polysome analysis shown above indicates that the primary defect caused by Rrp43p depletion is in 40S ribosome metabolism. For this reason we performed pulse–chase labeling and northern blot analysis of rRNA synthesis in normal and Rrp43p-depleted cells. The kinetics of rRNA processing were analyzed by pulse–chase labeling with [methyl-^{3}H]methionine using cells shifted from galactose to glucose medium for 8 h (Fig. 4). In control cells, [methyl-^{3}H]-labeled 27S and 20S pre-rRNAs were quickly chased to 25S and 18S rRNA, respectively. In these cells, 35S pre-rRNA is detected only at time 0 of the chase. In contrast, Rrp43p-depleted cells accumulated 35S pre-rRNA, which is indicative of an impairment in initial processing steps. In addition, Rrp43p-depleted cells accumulated

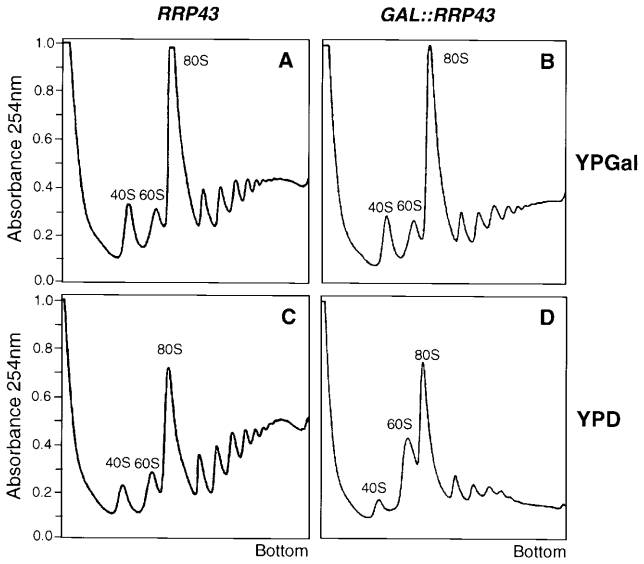

Figure 3. Rrp43p-depleted cells show defective polysome profiles. Polysome profiles were analyzed from strains W303-1a (*RRP43*) and DG458 (*GAL::RRP43*) by sedimentation through 15–50% sucrose gradients. Cultures were either grown in YPGal (**A** and **B**) or shifted to YPD for 12 h (**C** and **D**).

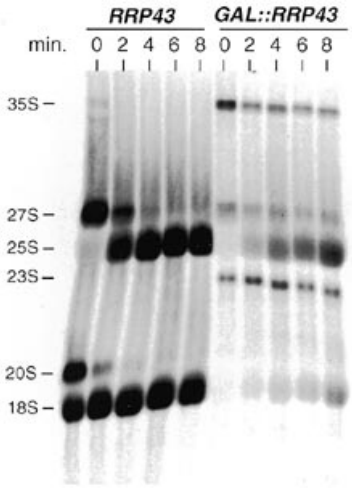

Figure 4. Pulse–chase labeling of rRNA synthesis in Rrp43p-depleted cells. Pulse–chase labeling with [methyl-^{3}H]methionine was performed in W303-1a (*RRP43*) and DG458 (*GAL::RRP43*) cells shifted from SCgal to SCglu lacking methionine for 8 h. RNA samples were collected every 2 min. An aliquot of 1 OD_{260} of total RNA was loaded in each lane. See Materials and Methods for details.

a 23S aberrant pre-rRNA. The status of 27S and 20S pre-rRNAs in Rrp43p-depleted cells, which are the precursors of 25S and 18S rRNAs, respectively, was also indicative of processing defects. Specifically, 27S pre-rRNA accumulated to abnormal levels in Rrp43p-depleted cells and 20S pre-rRNA levels were remarkable in being undetectable. Maturation of 25S and 18S rRNAs was significantly slowed, although 18S rRNA synthesis was more severely affected. An unusual feature of the rRNA processing defect in Rrp43p-depleted cells was the persistence of the 23S, 35S and 27S pre-rRNAs during the duration of the 8 min chase. These results strongly suggest that in addition to the maturation of 5.8S rRNA (7), Rrp43p is also required for processing steps leading to the synthesis of 25S and 18S rRNAs.

Steady-state pre-rRNA levels were analyzed from control and Rrp43p-depleted cells after shift to glucose medium for up to 12 h. Total RNA was isolated and submitted to northern hybridization with oligonucleotide probes specific for the 5′ ETS, ITS1, 5.8S rRNA and ITS2 (Fig. 1). The series of pre-rRNA processing defects detected by pulse–chase labeling was confirmed by the results obtained with northern blot analysis. Rrp43p-depleted cells accumulated 35S, 27S and 23S pre-rRNAs and were impaired in the synthesis of 20S pre-rRNA (Fig. 5). The decrease in the level of 20S pre-rRNA correlates with the appearance of the 23S pre-rRNA (Fig. 5B). The 23S aberrant pre-rRNA, which may be an intermediate along an alternative pathway to 18S rRNA (1,25), originates from direct cleavage of 35S pre-rRNA at site A_3 and contains the 5′ ETS, 18S rRNA and the ITS1 region upstream of site A_3. However, in Rrp43p-depleted cells, probes A and B detected more 23S than probe C (Fig. 5), indicating that most of this 23S pre-rRNA lacks the sequence between sites A_2 and A_3. These results, then, suggest that cleavage at A_2 is not severely impaired by Rrp43p depletion. No accumulation of the $27SA_2$ pre-rRNA was observed (Fig. 5C). Accumulation of a 7S pre-rRNA and the appearance of longer forms of 5.8S rRNA (5.8S* in Fig. 5D) were detected with probe D, which is complementary to a sequence of the mature 5.8S rRNA. According to a previous report (7), the longer 5.8S forms contain extended 3′-ends. Another unusual fragment was detected by probe E (Fig. 5E), which hybridizes within ITS2 between sites C_2 and E (Fig. 1). Probe E is complementary to a sequence adjacent to the 3′-end of mature 5.8S rRNA and, thus, can specifically detect 5.8S rRNA species with unprocessed 3′-ends. Since both probes D and E detect 5.8S rRNAs with extended 3′-ends, the 5.8S* and C_2/? bands (Fig. 5D and E) probably contain the same type of unprocessed intermediates. However, since probe E hybridizes between sites C_2 and E, it will detect any low molecular weight band containing this region of ITS2. In addition to the accumulation of normal and aberrant pre-rRNAs, Rrp43p-depleted cells also accumulated a fragment excised from the 5′ ETS (Fig. 5A, 5′/A_0), which most probably extends from the 5′-end to site A_0.

DISCUSSION

Nip7p was found both in the nucleolus and associated with free 60S ribosomal subunits in *S.cerevisiae* (16). Nip7p-depleted cells are deficient in 60S subunits and display pre-rRNA processing defects that include accumulation of 27S pre-rRNA (16). Rrp43p was isolated in a two-hybrid screen using Nip7p as bait. Biochemical analysis, showing that Nip7p co-purifies with a protein A–Rrp43p fusion, further supports an *in vivo* Nip7p–Rrp43p interaction (Zanchin and Goldfarb, in press). Rrp43p shares sequence homology with the RNase PH/PNPase family of ribonucleases (7,12) and has been identified as a component of the exosome complex whose subunits are required for processing of 5.8S rRNA (7). The two-hybrid and biochemical results indicate that Nip7p and Rrp43p interact either directly or indirectly via a common binding partner. The fact that both Nip7p and Rrp43p have been implicated in 60S biogenesis also suggested a possible functional interaction. Here, we present data

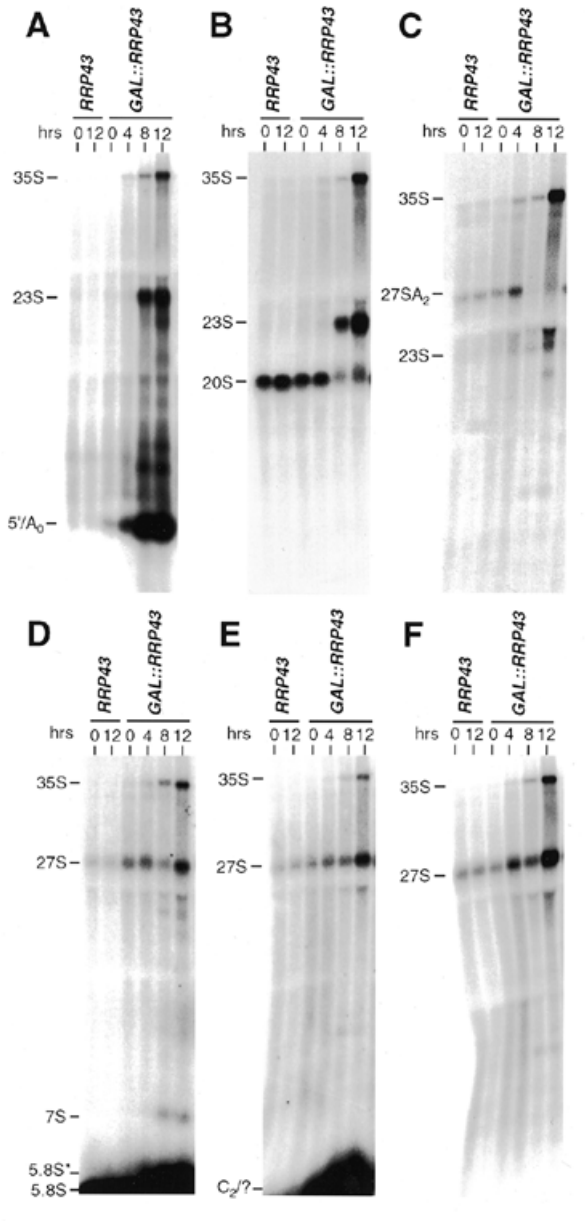

Figure 5. Analysis of pre-rRNA steady-state levels in Rrp43p-depleted cells. RNA was analyzed from strain W303-1a (*RRP43*) at times 0 and 12 h after transfer to YPD and from strain DG458 (*GAL*::*RRP43*) at times 0, 4, 8 and 12 h after transfer to YPD. Equivalent amounts of total RNA were loaded in each lane. (**A**) Probe A, complementary to sequences upstream of site A_0 in the 5′ ETS; (**B**) probe B, complementary to a region downstream of the 18S rRNA 3′-end/upstream of site A_2 in ITS1; (**C**) probe C, complementary to sequences between sites A_2 and A_3 in ITS1; (**D**) probe D, complementary to sequences in the 5.8S rRNA; (**E**) probe E, complementary to sequences between sites C_2 and E; (**F**) probe F, complementary to sequences between sites C_1 and C_2 in ITS2. See Materials and Methods and Figure 1 for details.

that confirm the role of Rrp43p in 5.8S maturation (7), but also provide new information implicating Rrp43p in other 35S pre-rRNA processing steps. One of the most interesting results is the strong inhibition of 18S rRNA synthesis observed in Rrp43p-depleted cells. This defect leads to a severe deficiency in the 40S subunit.

Regarding processing of the 60S subunit rRNAs, Rrp43p depletion resulted in accumulation of 7S pre-rRNA and 5.8S rRNAs with extended 3′-ends, which are the same type of defects as previously reported for Rrp43p-deficient cells (7), and stabilization of 27S pre-rRNAs. Accumulation of 27S pre-rRNA, which is also observed in Nip7p-depleted cells (16), provides evidence that may explain the Nip7p–Rrp43p interaction detected in the two-hybrid system. This result suggests that Rrp43p may interact transiently with or form stable complexes with Nip7p that are independent with its association with other exosome subunits. Alternatively, Nip7p may associate transiently with the exosome in the nucleus or cytoplasm. In any case, the processing defects associated with Rrp43p and Nip7p deficiencies are consistent with an Rrp43p–Nip7p complex functioning in 27S pre-rRNA processing. It is unclear, however, whether these factors are directly involved in the endonucleolytic cleavage of ITS2 because Rrp43p is a putative 3′→5′ exoribonuclease and the biochemical function of Nip7p is not known (7,16).

The initial processing of 35S pre-rRNA involves excision of the 5′ ETS followed by cleavage of ITS1 at A_2 (1). Inhibition of these early processing steps is typical of factors that are required for 18S rRNA synthesis and 40S subunit biogenesis (1). Rrp43p depletion also results in the persistence of 35S pre-rRNA and the stable accumulation of an aberrant 23S pre-rRNA, which implicates Rrp43p in the processing of the 5′ ETS, although there is no evidence of a direct catalytic role for Rrp43p in the cleavages at sites A_0 and A_1. The 23S aberrant pre-rRNA is formed by direct cleavage of 35S pre-rRNA at A_3 (1,25). However, most of the 23S pre-rRNA detected in Rrp43p-depleted cells does not seem to contain the region between sites A_2 and A_3 (Fig. 5), indicating that processing at A_2 occurs relatively efficiently without Rrp43p. Rrp43p has not been shown to have catalytic RNase activity, but the accumulation of aberrant precursors, such as the 23S pre-rRNA species, is consistent with a role for Rrp43p in the degradation of off-pathway pre-rRNAs. In addition, the accumulation of a fragment excised from the 5′ ETS ($5'/A_0$) in Rrp43p-depleted cells supports the hypothesis that Rrp43p is required for the degradation of excised spacer sequences. Interestingly, accumulation of the fragment $5'/A_0$ has been described in cells that are deficient for the exosomal subunit Rrp4p (11) and the putative RNA helicase Dob1p, which interacts genetically with Rrp4p (26). These results suggest that all of these proteins are required for the efficient degradation of the excised 5′ ETS.

The exosome was initially described as a complex of five 3′→5′ exoribonucleases that are necessary for 5.8S rRNA 3′-end formation (7). However, subsequent work has shown that certain exosomal subunits are not restricted to 5.8S rRNA processing. Rrp4p and Rrp41p/Ski6p also participate in mRNA degradation (15). In addition, the *ski6-2* allele of *RRP41*/*SKI6* accumulates a 60S subunit-derived 38S particle that contains a truncated 25S rRNA molecule and lacks 5.8S rRNA (13). Here, we show that in addition to the processing of 5.8S rRNA, Rrp43p is required for the efficient maturation of 18S and 25S rRNAs, for degradation of an excised spacer sequence and, possibly, also for degradation of aberrant pre-rRNAs. These results indicate that Rrp43p plays multiple roles in the metabolism of 35S pre-RNA.

ACKNOWLEDGEMENTS

We thank Nataliya Shulga for help with the figures. American Cancer Society grant B-104C (D.S.G.) supported this project.

REFERENCES

1 Lafontaine,D. and Tollervey,D. (1995) *Biochem. Cell Biol.*, **73**, 803–812.
2 Woolford,J.L.,Jr and Warner,J.R. (1991) In Broach,J.R., Pringle,J.R. and Jones,E.W. (eds), *The Molecular Biology of the Yeast Saccharomyces: Genome Dynamics, Proteins Synthesis and Energetics*. Cold Spring Harbor Laboratory Press, Cold Spring Harbor, NY, pp. 587–626.
3 Smith,C.M. and Steitz,J.A. (1997) *Cell*, **89**, 669–672.
4 Tollervey,D. and Kiss,T. (1997) *Curr. Opin. Cell Biol.*, **9**, 337–342.
5 Udem,S.A. and Warner,J.R. (1973) *J. Biol. Chem.*, **248**, 1412–1416.
6 Henry,Y., Wood,H., Morrissey,J.P., Petfalski,E., Kearsey,S. and Tollervey,D. (1994) *EMBO J.*, **13**, 2452–2463.
7 Mitchell,P., Petfalski,E., Shevchenko,A., Mann,M. and Tollervey,D. (1997) *Cell*, **91**, 457–466.
8 Stevens,A., Hsu,C.L., Isham,K.R. and Larimer,F.W. (1991) *J. Bacteriol.*, **173**, 7024–7028.
9 Elela,S.A., Igel,H. and Ares,M.,Jr (1996) *Cell*, **85**, 115–124.
10 Lygerou,Z., Allmang,C., Tollervey,D. and Séraphin,B. (1994) *Science*, **272**, 268–270.
11 Mitchell,P., Petfalski,E. and Tollervey,D. (1996) *Genes Dev.*, **10**, 502–513.
12 Mian,I.S. (1997) *Nucleic Acids Res.*, **25**, 3187–3195.
13 Benard,L., Carroll,K.R., Valle,C.P. and Wickner,R.B. (1998) *Mol. Cell. Biol.*, **18**, 2688–2696.
14 Briggs,M.W., Burkard,K.T.D. and Butler,J.S. (1998) *J. Biol. Chem.*, **273**, 13255–13263.
15 Anderson,J.S.J. and Parker,R. (1998) *EMBO J.*, **17**, 1497–1506.
16 Zanchin,N.I.T., Roberts,P., DeSilva,A., Sherman,F. and Goldfarb,D.S. (1997) *Mol. Cell. Biol.*, **17**, 5001–5015.
17 Sambrook,J., Maniatis,T. and Fritsch.,E.F. (1989) *Molecular Cloning: A Laboratory Manual*, 2nd Edn. Cold Spring Harbor Laboratory Press, Cold Spring Harbor, NY.
18 Gietz,R.D. and Sugino,A. (1988) *Gene*, **74**, 527–534.
19 Sherman,F. (1991) *Methods Enzymol.*, **194**, 3–21.
20 Sherman,F., Fink,G.R. and Hicks,J.B. (1986) *Laboratory Course Manual for Methods in Yeast Genetics*. Cold Spring Harbor Laboratory Press, Cold Spring Harbor, NY.
21 Güldener,U., Heck,S., Fiedler,T., Beinhauer,J. and Hegemann,J.H. (1996) *Nucleic Acids Res.*, **24**, 2519–2524.
22 Warner,J.R. (1991) *Methods Enzymol.*, **194**, 423–428.
23 Köhrer,K. and Domdey,H. (1991) *Methods Enzymol.*, **194**, 398–405.
24 Tollervey,D. (1987) *EMBO J.*, **6**, 4169–4175.
25 Hughes,J.M.X. and Ares,M.J. (1991) *EMBO J.*, **10**, 4231–4239.
26 De la Cruz,J., Kressler,D. Tollervey,D. and Linder,P. (1998) *EMBO J.*, **17**, 1128–1140.